Reexamination of 1,4-Hydride Exchange within the η^5-Naphthalenyl Complex [Mn(η^5-$C_{10}H_9$)$(CO)_3$] Establishes an Exchange Rate Intermediate between Those in the Cyclohexadienyl and Anthracenyl Analogues

Jacqueline M. Veauthier,[†] Albert Chow,[‡] Gideon Fraenkel,*[,‡] Steven J. Geib,*[,†] and N. John Cooper*[,†]

Departments of Chemistry, University of Pittsburgh, Pittsburgh, Pennsylvania 15260, and Ohio State University, Columbus, Ohio 43210

Received February 4, 2000

Magnetization transfer experiments establish that the η^5-naphthalenyl complex [Mn(η^5-$C_{10}H_9$)$(CO)_3$] participates in a 1,4-hydride shift reaction that involves exchange of the endo proton with the proton para to this position. Dynamic NMR studies establish that $\Delta G^{\ddagger}$ for this exchange is 21.0 kcal/mol at 298 K, intermediate between the previously reported exchange barriers of 34 kcal/mol in the benzene-derived complex [Mn(η^5-C_6D_6H)$(CO)_3$] and 14.6 kcal/mol for the anthracene-derived complex [Mn(η^5-$C_{14}H_{11}$)$(CO)_3$].

Introduction

We recently observed that the η^5-anthracenyl complex [Mn(η^5-$C_{14}H_{11}$)$(CO)_3$] (**1**), formed by protonation of the η^4-anthracene complex [Mn(η^4-$C_{14}H_{10}$)$(CO)_3$] (**2**$^-$) (Scheme 1), participates in a 1,4-hydride exchange with a surprisingly low $\Delta G^{\ddagger}$ of 14.6 kcal/mol.[1] This is dramatically lower than the established barrier of 34 kcal/mol for the parent benzene-derived complex [Mn(η^5-C_6D_6H)$(CO)_3$] (**3**-d_6),[2] and we proposed that this difference could be a consequence of a 1,4-hydride shift mechanism in which hydride migration to the metal is synchronous with deligation of the edge of the aromatic substituent fused to the dienyl ligand and that this generates a highly symmetric diene hydride intermediate.

Given the kinetic parameters for 1,4-hydride shifts in **3**-d_6 and **1**, we were surprised by a report that appeared while our work was in progress indicating that the barrier to the 1,4-hydride shift in the η^5-naphthalenyl complex [Mn(η^5-$C_{10}H_9$)$(CO)_3$] (**5**) occurs with an enthalpy of activation of 18.8 kcal/mol and an entropy of activation of 3.6 eu (corresponding to $\Delta G^{\ddagger} = 17.7$ kcal/mol at 298 K).[3] We would have anticipated activation parameters intermediate between those for **3**-d_6 and **1** and hence a higher $\Delta H^{\ddagger}$; since we have convenient access to **5** by a reductive activation/protonation sequence via [Mn(η^4-$C_{10}H_8$)$(CO)_3$] (**4**$^-$),[4] we have now reinvestigated the fluxionality of **5**. We have confirmed the existence of a metal-mediated 1,4-hydride shift in **5** and have determined kinetic parameters for this shift corresponding to an enthalpy of activation of 26.4 ± 1.3 kcal/mol and an entropy of activation of 18.1 ± 3.6 eu ($\Delta G^{\ddagger} = 21.0$ kcal/mol at 298 K). These parameters are intermediate between the data for **3**-d_6 and **1**; given the discrepancy with the literature, we now report details of our experiments.

Scheme 1

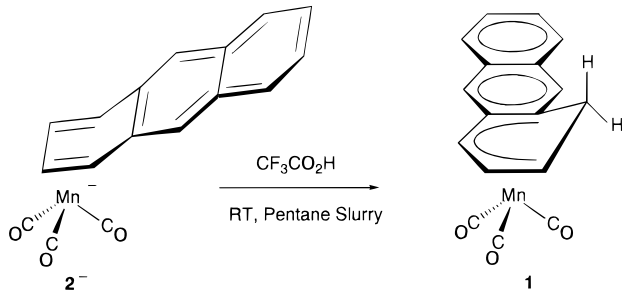

Experimental Section

General Procedures. All reactions and manipulations were carried out under an atmosphere of dry, oxygen-free nitrogen as described in a recent publication.[1]

Unless otherwise stated, all reagents were used as received. Trifluoroacetic acid (CF_3CO_2H) was purchased from Aldrich, and samples of [PPN][Mn(η^4-$C_{10}H_8$)$(CO)_3$] (PPN**4**) were prepared according to the method described by Thompson et al.[4]

Dynamic NMR. Variable-temperature ^{1}H NMR spectra were recorded on a Bruker AC 300 spectrometer at 300 MHz. Temperatures within the NMR probe were controlled by a Bruker variable-temperature unit, which was calibrated against ethylene glycol and boiling and freezing H_2O and found to be accurate to within 0.2 °C. Samples for variable-temperature NMR were prepared in $C_6D_5CD_3$ in 5 mm NMR tubes, degassed by several freeze/pump/thaw cycles, and then sealed under vacuum.

Population transfer studies were carried out as described previously.[1]

X-ray Crystallography. Crystals for X-ray diffraction studies were coated with fluorolube then mounted on a glass

[†] University of Pittsburgh.
[‡] Ohio State University.

(1) Veauthier, J. M.; Chow, A.; Fraenkel, G.; Geib, S. J.; Cooper, N. J. *Organometallics* **2000**, *19*, 661.
(2) Lamanna, W.; Brookhart, M. *J. Am. Chem. Soc.* **1980**, *102*, 3490.
(3) Georg, A.; Kreiter, C. G. *Eur J. Inorg. Chem.* **1999**, 651.
(4) Thompson, R. L.; Lee, S.; Rheingold, A. L.; Cooper, N. J. *Organometallics* **1991**, *10*, 1657.

10.1021/om000102y CCC: $19.00
Publication on Web 08/17/2000

Scheme 2

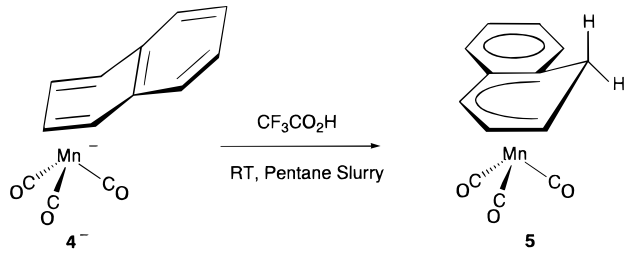

fiber and coated with epoxy. X-ray data were collected on a Siemens P3 diffractometer using graphite-monochromatized Mo Kα radiation ($\lambda = 0.71073$ Å). Data processing and graphics were done with the Siemens SHELXTL package program. All non-hydrogen atoms were located and refined anisotropically. All hydrogen atoms were located and refined isotropically.

Microanalysis. Microanalyses were performed by Atlantic Microlab, Norcross, GA.

Preparation of [Mn(η^5-$C_{10}H_9$)$(CO)_3$]. To a slurry of 0.349 g (0.433 mmol) of [PPN][Mn(η^4-$C_{10}H_8$)$(CO)_3$] in 20 mL of *n*-pentane was added 34 μL (0.44 mmol) of CF_3CO_2H. A yellow-orange pentane solution formed, while much of the yellow [PPN][Mn(η^4-$C_{10}H_8$)$(CO)_3$] remained behind. IR spectra of the orange-yellow solution confirmed the presence of a neutral complex (IR: $\nu_{C\equiv O}$, *n*-pentane, 2020 (vs), 1945 (vs), 1925 (vs) cm^{-1}). The infrared spectrum also contained a band at 1700 (m) cm^{-1} assigned to [PPN][CF_3CO_2] (which is sparingly soluble in pentane). Slow cooling of the pentane solution to −80 °C gave 0.035 g of small X-ray quality orange crystals of [Mn(η^5-$C_{10}H_9$)$(CO)_3$] (0.131 mmol, 30%). ^{1}H NMR (300 MHz, $C_6D_5CD_3$, 297 K): δ 6.79 (d, $J_{6-7} = 8.00$ Hz, 1H, H_6), 6.73 (t, $J_{7-8}/J_{7-6} = 8.00$ Hz, 1H, H_7), 6.61 (t, $J_{8-9}/J_{8-7} = 8.00$ Hz, 1H, H_8), 6.57 (d, $J_{8-9} = 8.00$ Hz, 1H, H_9), 5.88 (d, $J_{4-3} = 5.50$ Hz, 1H, H_4), 4.70 (t, $J_{3-4}/J_{3-2} = 5.50$ Hz, 1H, H_3), 2.89 (dd, $J_{exo-endo} = 14.5$ Hz, $J_{endo-2} = 5.50$ Hz, 1H, H_{endo}), 2.84 (t, J_{2-3} / $J_{2-endo} = 5.50$ Hz, 1H, H_2), 2.32 (d, $J_{exo-endo} = 14.5$ Hz, 1H, H_{exo}). Anal. Calcd for $C_{13}H_9MnO_3$: C, 58.23; H, 3.38. Found: C, 58.15; H, 3.45.

Results and Discussion

Our group previously reported the preparation of [Mn(η^5-$C_{10}H_9$)$(CO)_3$] by a route in which K[Mn(η^4-$C_{10}H_8$)$(CO)_3$] is formed in situ and addition of CF_3CO_2H gives [Mn(η^5-$C_{10}H_9$)$(CO)_3$] in 39% yield.[4] We have modified this procedure slightly by first isolating the η^4-naphthalene complex as a PPN^+ salt, which can then be protonated; this provides cleaner samples of the η^5-naphthalenyl complex, capable of forming diffraction grade crystals, in yields similar to that provided by the original preparation.

Reaction of [PPN][Mn(η^4-$C_{10}H_8$)$(CO)_3$] with CF_3CO_2H and Synthesis and Spectroscopic Characterization of [Mn(η^5-$C_{10}H_9$)$(CO)_3$]. Protonation of **4**$^-$ to give [Mn(η^5-$C_{10}H_9$)$(CO)_3$] (**5**, 30%) was achieved by addition of CF_3CO_2H to an orange slurry of [PPN][Mn(η^4-$C_{10}H_8$)$(CO)_3$] in *n*-pentane (Scheme 2). The room-temperature ^{1}H NMR spectrum of **5** compares well with the spectra reported by Thompson et al.[4] Full assignments are listed in the Experimental Section; the endo and exo protons have been assigned according to the predictions of the Karplus[5] relationship concerning the dihedral (or torsional) angle between the protons vicinal to each other (see below) and the corresponding coupling constant.

Structural Characterization of [Mn(η^5-$C_{10}H_9$)$(CO)_3$]. The modified synthetic procedure used for **5** in this work gave access to clean samples that form diffraction grade crystals. Structural characterization as described in the Experimental Section then allowed us to establish the molecular structure shown in Figure 1. All atoms, including hydrogen atoms, were experimentally located and refined, allowing us to obtain experimental data for key structural parameters such as the torsional angle between the C(1)−H_{endo} bond and the C(2)−H(2) bond, 38.4°. Sweigart and co-workers recently reported a diffraction study of **5** that agrees with our data.[6] They did not, however, locate and refine the hydrogen atoms, and since the positions of these atoms could be important with regard to the fluxionality of **5**, we provide details of our diffraction study. Selected bond lengths and angles for **5** are listed in Table 2.

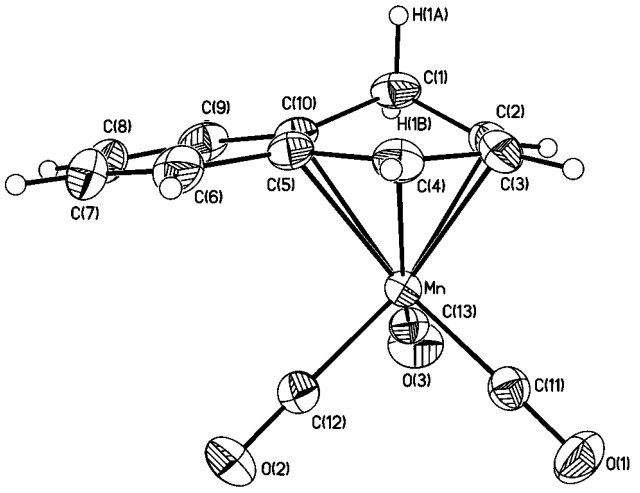

Figure 1. ORTEP drawing of [Mn(η^5-$C_{10}H_9$)$(CO)_3$] (35% probability ellipsoids).

Complex **5** has a nearly planar dienyl fragment with the aromatic ring attached at the first two atoms following the sp^3 carbon and bent slightly below the plane (8.9°). The cyclohexadienyl ring is folded about C(2)−C(10) (dihedral angle of 36.0(2)°; cf. 33.4(3)° for [Mn(η^5-$C_{14}H_{11}$)$(CO)_3$],[1] 42° for [Mn(η^5-C_6H_7)$(CO)_3$],[7] and a range of 39.6−29.6° for other substituted dienyl complexes[8]).

The torsion angle between the C(1)−H_{exo} and C(2)−H_{ortho} is 81.2° and that between C(1)−H_{endo} and C(2)−H_{ortho} is 38.4°, consistent with the expectations established by the NMR data that the H_{exo}/H_{ortho} angle must be close to 90° and that the H_{endo}/H_{ortho} angle must be much smaller.

(5) Karplus, M. *J. Chem. Phys.* **1959**, *30*, 11.
(6) Sun, S. H.; Dullaghan, C. A.; Carpenter, G. B.; Sweigart, D. A.; Lee, S. S.; Chung, Y. K. *Inorg. Chim. Acta* **1997**, *262*, 213.
(7) Churchill, M. R.; Scholer, F. R. *Inorg. Chem.* **1969**, *8*, 1950.
(8) (a) Ittel, S. D.; Whitney, J. F.; Chung, Y. K.; Williard, P. G.; Sweigart, D. A. *Organometallics* **1988**, *7*, 1323. (b) Ryan, W. J.; Peterson, P. E.; Cao, Y.; Williard, P. G.; Sweigart, D. A.; Baer, C. D.; Thompson, C. F.; Chung, Y. K.; Chung, T.-M. *Inorg. Chim. Acta* **1993**, *211*, 1. (c) Reau, R.; Reed, R. W.; Dahan, F.; Bertrand, G. *Organometallics* **1993**, *12*, 1501. (d) Lee, T.; Yu, H. B.; Chung, Y. K.; Hallows, W. A.; Sweigart, D. A. *Inorg. Chim. Acta* **1994**, *224*, 147. (e) Rose-Munch, F.; Le Corre-Susanne, C.; Balssa, F.; Rose, E.; Vaisserman, J.; Licandro, E.; Papagni, A.; Maiorana, S.; Meng, W.; Stephenson, G. R. *J. Organomet. Chem.* **1997**, *545*−*546*, 9. (f) Balssa, F.; Gagliardini, V.; Le Corre-Susanne, C.; Rose-Munch, F.; Rose, E.; Vaisserman, J. *Bull. Soc. Chim. Fr.* **1997**, *134*, 537. (g) Rose-Munch, F.; Gagliardini, V.; Renard, C.; Rose, E. *Coord. Chem. Rev.* **1998**, *178*−*180*, 249. (h) Rose, E.; Le Corre-Susanne, C.; Rose-Munch, F.; Renard, C.; Gagliardini, V.; Teldji, F.; Vaissermann, J. *Eur. J. Inorg. Chem.* **1999**, *3*, 421.

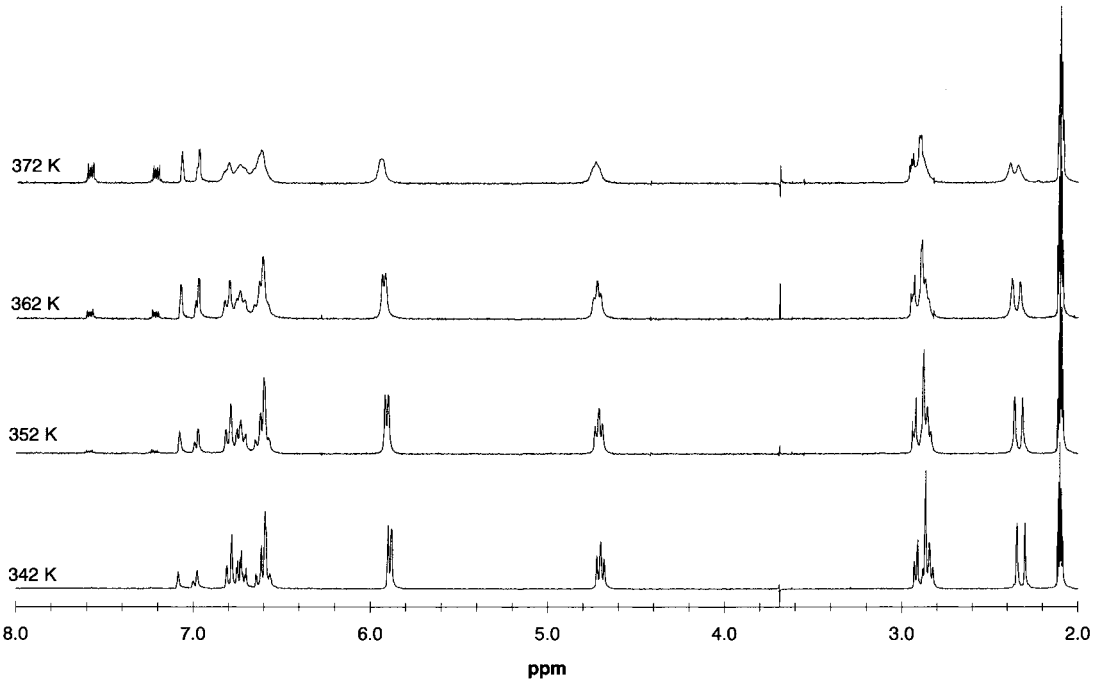

Figure 2. Variable-temperature ^{1}H NMR spectra of [Mn(η^5-$C_{10}H_9$)$(CO)_3$] (300 MHz, $C_6D_5CD_3$).

Table 1. Crystal Data, Data Collection Parameters, and Agreement Factors for [Mn(η^5-$C_{10}H_9$)$(CO)_3$]

formula	$C_{13}H_9MnO_3$
fw	268.14
temp, K	208 (2) K
wavelength, Å	0.71073
crystal system	monoclinic
space group	$P2_1/c$
a, Å	7.130(3)
b, Å	13.140(5)
c, Å	12.440(5)
β, deg	105.00(3)
V, Z, Å^3	1125.7(8), 4
ρ(calcd), Mg/m^3	1.582
μ, mm^{-1}	1.163
F(000)	544
cryst size, mm	0.35 × 0.35 × 0.35
θ range, deg	2.30−25.99
limiting indices	$-5 \le h \le 8$, $-11 \le k \le 16$, $-15 \le l \le 14$
no. of reflns collected	2390
no. of ind reflns	2214 (R_{int} = 0.0236)
abs corr	empirical
refinement method	full-matrix least squares of F^2
no. of data/restraints/params	2214/0/190
goodness of fit on F^2	1.054
final R indices [$I>2\sigma(I)$]	R1 = 0.0399, wR2 = 0.0989
R indices (all data)	R1 = 0.0546, wR2 = 0.1072
largst diff peak and hole, e Å^{-3}	0.538 and −0.244

Variable-Temperature ^{1}H NMR Spectra of [Mn(η^5-$C_{10}H_9$)$(CO)_3$]. Consistent with our previous observations,[4] lines in the ^{1}H NMR spectrum of **5** are sharp and there is no room-temperature evidence of fluxionality in **5**. At elevated temperatures, however, line broadening becomes observable (Figure 2): at 342 K, some line broadening becomes noticeable and is more pronounced between 352 and 362 K; at 372 K, coupling between the protons in **5** is almost completely unresolved. The temperature-dependent changes are fully reversed when the sample is cooled back to room temperature. It was not feasible to examine the spectra at higher temperatures due to the onset of thermal decomposition of **5**.

Table 2. Selected Bond Lengths (Å) and Angles (deg) within [Mn(η^5-$C_{10}H_9$)$(CO)_3$

Mn−C(11)	1.785(3)	Mn−C(4)	2.121(3)
Mn−C(12)	1.807(3)	Mn−C(3)	2.129(3)
Mn−C(13)	1.808(3)	Mn−C(2)	2.183(3)
Mn−C(5)	2.260(3)	Mn−C(10)	2.395(3)
O(1)−C(11)	1.149(4)	C(2)−C(3)	1.390(5)
O(2)−C(12)	1.146(4)	C(3)−C(4)	1.402(5)
O(3)−C(13)	1.150(4)	C(4)−C(5)	1.437(5)
C(1)−C(2)	1.504(5)	C(5)−C(6)	1.417(5)
C(1)−C(10)	1.509(5)	C(9)−C(10)	1.417(5)
C(1)−H(1A)	0.94(4)	C(5)−C(10)	1.421(4)
C(1)−H(1B)	0.91(4)		
C(11)−Mn−C(12)	87.21(1)	O(1)−C(11)−Mn	178.7(3)
C(11)−Mn−C(13)	94.41(1)	O(2)−C(12)−Mn	179.3(3)
C(12)−Mn−C(13)	96.99(1)	O(3)−C(13)−Mn	177.4(3)
C(2)−C(1)−C(10)	106.5(3)	H(1A)−C(1)−H(1B)	106(3)

Magnetization Transfer and NOE Difference Spectra of [Mn(η^5-$C_{10}H_9$)$(CO)_3$].[9] To determine the origin of the line broadening in ^{1}H NMR spectra of **5** at elevated temperatures, we performed magnetization transfer experiments that generated NOE difference spectra of **5** at 297 and 327 K. These were obtained by irradiation of one resonance of the spectrum followed by application of a $\pi/2$ observation pulse to record the FID. If exchange occurs with the irradiated proton, magnetization will be transferred from the nucleus of the irradiated proton to one or more other protons in the system, and this will be observed as a change in signal strength wherever exchange occurs.

Magnetization transfer is typically observable at exchange rates below those at which exchange results in broadening of absorption mode lines. NOE difference spectra of **5** at 297 K provide no evidence for exchange at ambient temperature, but exchange was observable at 327 K (Figure 3). A pairwise exchange

(9) (a) Sanders, J. K.; Hunter, B. K. In *Modern NMR Spectroscopy: A Guide for Chemists*; Oxford University Press: New York, 1990; Chapters 1−3, 6, and 17. (b) Noggle, J. H.; Schirmer, R. E. In *The Nuclear Overhauser Effect*; Academic Press: New York, 1971; Chapters 1 and 7. (c) Forsen, S.; Hoffman, R. A. *J. Chem. Phys.* **1963**, *39*, 2892.

Scheme 3

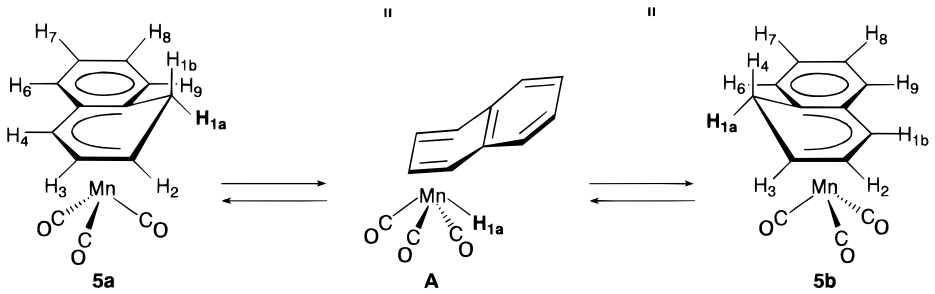

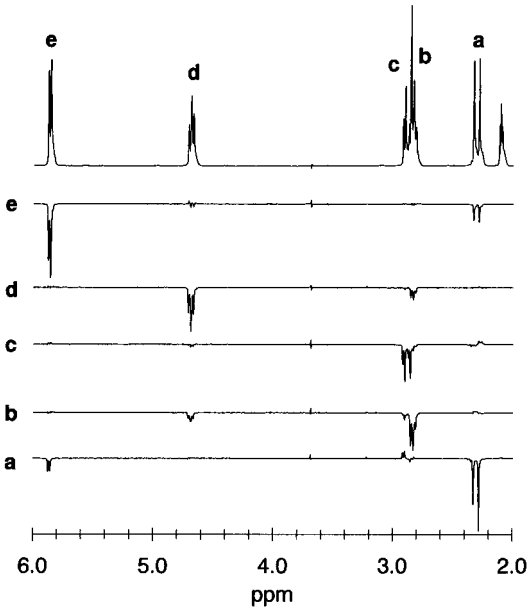

Figure 3. NOE difference spectra of $[Mn(\eta^5\text{-}C_{10}H_9)(CO)_3]$ at 327 K (300 MHz, $C_6D_5CD_3$). The difference spectra are labeled with letters that correspond to the peak being irradiated.

process is observed: irradiation at 2.32 δ (spectrum **a**) also inverts the resonance at 5.88 δ, and analogously irradiation at 5.88 δ (spectrum **e**) inverts the peak at 2.32 δ (magnetization is transferred between the exo and para protons of **5**); irradiation at 2.84 δ (spectrum **b**) inverts the peak at 4.70 δ and irradiation at 4.70 δ (spectrum **d**) inverts the peak at 2.84 δ (magnetization is transferred between the ortho and meta protons). If, however, the peak at 2.89 δ is irradiated, no other peak inverts (spectrum **c**): magnetization is not transferred from the endo proton to any other proton. It was not possible to access irradiation bandwidths sufficiently narrow enough to irradiate single proton resonances in the aromatic region, but when a $\pi/2$ pulse is applied to the aromatic region of the spectrum, only peaks in that region invert; it is clear that each of the protons in **5**, with the exception of the endo hydrogen of the methylene group, is exchanging environments with one other proton in **5**. The observed exchange pattern is consistent with a metal-mediated process in which the endo hydrogen moves down to the metal and then back up into a symmetric position on the ring (Scheme 3) in a reaction similar to the 1,4-hydride exchange that we have recently established occurs in $[Mn(\eta^5\text{-}C_{14}H_{11})(CO)_3]$.[1]

Quantitative Analysis of 1,4-Hydride Shift in $[Mn(\eta^5\text{-}C_{10}H_9)(CO)_3]$. The identification of the exchange process in **5** established through magnetization transfer experiments allowed simulations of the dynamic ^{1}H NMR spectra to determine the free energy barrier to activation for the 1,4-hydride shift in **5**. Spectra were acquired between 342 and 372 K at 5 K intervals, and line shapes for the regions between 6.5 and 2.0 δ were simulated for each spectrum using the DNMR3 program[10] (see Supporting Information for simulated spectra). The simulated exchange rates at each temperature and the corresponding activation energy for the 1,4-hydride migration between the two equivalent sites on the naphthalene ligand are summarized in Table 3. The Eyring plot[11] of the data shown in Figure 4 establishes an enthalpy of activation for the migration of 26.4 $\pm$ 1.3 kcal/mol and an entropy of activation of 18.1 $\pm$ 3.6 eu.

Table 3. Rates of Exchange for 1,4-Hydride Shift in $[Mn(\eta^5\text{-}C_{10}H_9)(CO)_3]$ Calculated from Line Shape Analysis

T (K)	k (s^{-1})	$\Delta G^{\ddagger}$ (kcal/mol)
342	0.75	20.0
347	1.5	20.1
352	3.0	20.0
357	5.0	19.9
362	9.0	19.7
367	13.0	19.8
372	18.0	19.8

Comparison of 1,4-Hydride Shift Parameters Observed for 5 with Literature Data. The enthalpy and entropy of activation that we have established for 1,4-hydride shift in **5** differ by more than experimental error from the corresponding data reported by Georg and Kreiter,[3] and we have examined our data analysis carefully to be sure that our figures our correct; we are confident that they are. There is insufficient data or experimental details available in the literature to determine the source of the discrepancy between our data and the literature data, but we note that the rates reported in the literature correspond to line widths of 12.2 Hz for peaks such as the 5.9 δ peak in the 348 K spectrum (this compares to 8.4 Hz in our simulated spectrum at 347 K) and 17.4 Hz in the 358 K spectrum (this compares to 9.3 Hz in our simulated spectrum at 357 K). This is markedly larger than the line widths that we observe as shown in Figure 5. In spectroscopy, experimental deviations from ideal conditions almost invariably increase line widths (rather than decrease them), and we conclude that our data are inherently more likely to be accurate.

The activation barrier that we have determined for the 1,4-hydride shift within the η^5-naphthalenyl com-

(10) The DNMR3 program (http://www.arl.hpc.mil/PET/cta/ccm/software/qcpe/QCPE2/index.html) was used to simulate the ^{1}H NMR spectra: (a) Kleier, D. A.; Binsch, G. *QCPE* **1970**, *11*, 165. (b) Binsch, G.; Kessler, H. *Angew. Chem., Int. Ed. Engl.* **1980**, *19*, 411.

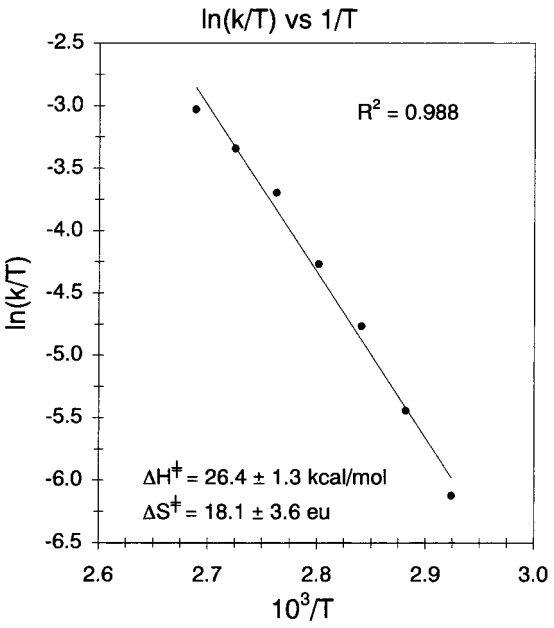

Figure 4. Eyring plot for the 1,4-hydride shift in [Mn(η^5-$C_{10}H_9$)$(CO)_3$] in $C_6D_5CD_3$. The errors reported in the activation parameters are based on the method of least squares and are calculated from the standard deviations in the slope and *y*-intercept.

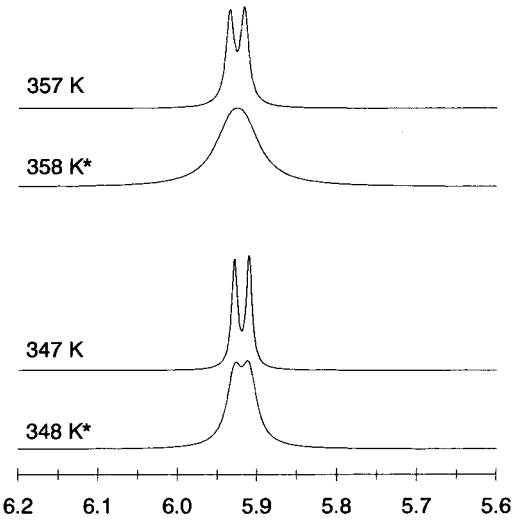

Figure 5. Comparison of calculated line shapes for [Mn(η^5-$C_{10}H_9$)$(CO)_3$] (showing the resonance for the proton para to the methylene group), this paper vs Georg et al. (*).

plex **5** is intermediate between the barrier established for the corresponding 1,4-hydride shift in the anthracenyl complex **1** and that for the fluxional process in the parent cyclohexadienyl complex **3**-d_6, as illustrated by the bar graph in Figure 6.

The data are not strictly comparable (the fluxional process in **3**-d_6 is not restricted to a 1,4-shift since the literature data on [Mn(η^5-C_6D_6H)$(CO)_3$] establish that the exo hydrogen can scramble to other carbon atoms in the ring[2]), but the trend in activation energies observed in Figure 6 does seem reasonable. The addition of a single aromatic ring to the parent cyclohexadienyl system **3**-d_6 significantly decreases $\Delta G^{\ddagger}$ from 34 to 21.0 kcal/mol, while the addition of a second aromatic ring produces only a modest further reduction of $\Delta G^{\ddagger}$ to 14.6 kcal/mol. The precise origin of the effect of an aromatic

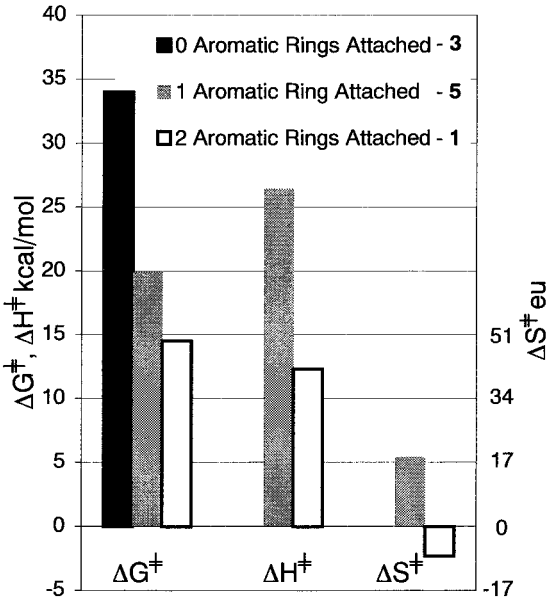

Figure 6. Comparison of activation parameters for the 1,4-hydride shift in [Mn(η^5-$C_{10}H_9$)$(CO)_3$] in $C_6D_5CD_3$. The entropy axis has been scaled such that the entropy bars give $-T\Delta S^{\ddagger}$ at 298 K when read against the $\Delta G^{\ddagger}$, $\Delta H^{\ddagger}$ axis. $\Delta G^{\ddagger}$ for **3** is at 418 K; $\Delta G^{\ddagger}$ values for **5** and **1** are calculated at 298 K.

substituent on the barrier to the 1,4-hydride shift is unclear and is under investigation in our group, but is comparable to the well-documented indenyl effect[12] for ligand substitution in the isoelectronic η^5-cyclopentadienyl complexes of manganese tricarbonyl. An analogous effect was recently invoked by Son et al.[13] to explain why CO substitution in **5**, which is proposed to occur via a ring-slipped intermediate, is accelerated in the naphthalenyl case when compared to CO substitution in the relatively inert η^5-cyclohexadienyl complexes.

There is an intriguing change in activation entropies for the 1,4-hydride shifts on going from **5** to **1**, with a change from a positive 18 eu to a modestly negative −7.7 eu (Figure 6), indicating that the hydride shift in **5** has a less ordered transition state than the hydride shift in **1**. The significance of this is unclear, but it is certainly consistent with our previous suggestion that the remarkably low barrier observed for 1,4-hydride shift in **1** may reflect a highly symmetric transition state with maximal aromatic stabilization.

The availability of diffraction data for complexes **1** and **5** in which the hydrogen atoms are experimentally located and refined allows us to rule out any unusual ground-state interaction between the endo C−H and the metal center[14] that would influence the course of, or the activation parameters for, 1,4-hydride shift within **1** and **5**.

(11) (a) Sandstrom, J. In *Dynamic NMR Spectroscopy*; Academic Press: London, 1982; Chapter 7. (b) Glasstone, S.; Laidler, K.; Eyring, H. In *The Theory of Rate Processes*; McGraw-Hill: New York, 1941; p 195. (c) Eyring, H. *Chem. Rev.* **1935**, *17*, 65.

(12) (a) Rerek, M. E.; Ji, L.-N.; Basolo, F. *J. Chem. Soc., Chem. Commun.* **1983**, 1208. (b) Ji, L.-N.; Rerek, M. E.; Basolo, F. *Organometallics* **1984**, *3*, 740. (c) O'Connor, J. M.; Casey, C. P. *Chem. Rev.* **1987**, *87*, 307. (d) Merola, J. S.; Kacmarcik, R. T.; Van Engen, D. *J. Am. Chem. Soc.* **1986**, *108*, 329, and references therein. (e) Crabtree, R. H. In *The Organometallic Chemistry of the Transition Metals*, 2nd ed.; John Wiley & Sons: New York, 1994; Chapters 4 and 5.

(13) Son, S. U.; Paik, S.-J.; Lee, I. S.; Lee, Y.-A.; Chung, Y. K. *Organometallics* **1999**, *18*, 4114.

Acknowledgment. This work was financially supported by the NSF through grant nos. CHE 9632202 (N.J.C.) and CHE 9615116 (G.F.).

(14) The metal-to-hydrogen distance Mn···H_{endo} is 3.23 (1) Å in **1** and 3.13 (1) Å in **5**.

Supporting Information Available: Complete X-ray crystallographic data for **5** and complete dynamic ^{1}H NMR spectra for the line shape analysis of complex **5** are available at http://www.pubs.acs.org.

OM000102Y